Laser-Field-Free Molecular Orientation

Akihisa Goban, Shinichirou Minemoto, and Hirofumi Sakai[*]
Department of Physics, Graduate School of Science, The University of Tokyo, 7-3-1 Hongo, Bunkyo-ku, Tokyo 113-0033, Japan

(Received 4 April 2008; published 30 June 2008)

We demonstrate laser-field-free molecular orientation with the combination of a moderate electrostatic field and an intense nonresonant rapidly turned-off laser field, which can be shaped with the plasma shutter technique. We use OCS (carbonyl sulfide) molecules as a sample. Molecular orientation is adiabatically created in the rising part of the laser pulse, and it is found to revive at around the rotational period of an OCS molecule with the same degree of orientation as that at the peak of the laser pulse in the virtually laser-field-free condition. This accomplishment means that a new class of molecular sample has become available for various applications.

DOI: 10.1103/PhysRevLett.101.013001 PACS numbers: 33.80.Rv, 33.15.Bh, 42.50.Wk

Molecular manipulation techniques based on laser technologies and their applications are among hot topics both in physics and in chemistry over the past decade [1,2]. A sample of aligned or oriented molecules can serve as an ideal anisotropic quantum system to investigate not only stereodynamics in chemical reactions [3] but also "electronic stereodynamics" in molecules as pointed out by Herschbach [4]. Recently, molecular alignment and orientation techniques attracted widespread attention also in the fields of ultrafast molecular imaging [5], attosecond science [6], and surface science [7].

Concerning molecular orientation, Friedrich and Herschbach proposed that orientation in a moderate electrostatic field can be greatly enhanced by combining an intense nonresonant laser field [8,9]. Based on this combined-field technique, both one- and three-dimensional orientations have already been demonstrated in the adiabatic regime by the authors [10–12]. With this technique, the molecular orientation can be maintained for a relatively long period of typically a few nanoseconds in the presence of an intense laser field.

On the other hand, an intense laser field can modify the physics and/or chemistry involved and can be an obstacle in some applications in precision spectroscopy, photoelectron spectroscopy, and so on. Therefore, the realization of laser-field-free or nonadiabatic molecular orientation has been desired for a long time. Although most of the recent theoretical proposals for this goal are based on the use of an intense half-cycle pulse in the terahertz region as a quasi-electrostatic field [13,14], laser-field-free molecular orientation along those schemes has remained unrealized. We recently proposed a technique to achieve nonadiabatic laser-field-free molecular orientation with the combination of an electrostatic field and an intense nonresonant rapidly turned-off laser field [15]. Here we report clear evidence of nonadiabatic laser-field-free molecular orientation based on our technique. As a sample, we employ OCS (carbonyl sulfide) molecules with a moderate permanent dipole moment $\mu_0 = 0.71$ D [16].

The anisotropic polarizability interaction of the induced dipole moment of a molecule with an intense nonresonant laser field produces a double-well potential along the polarization direction, which creates a pendular state where the molecular axis librates around the polarization. The pendular energy levels are formed in the potential with nearly degenerate tunneling doublet states of opposite parity. If the molecule is polar, the introduction of an electrostatic field couples the components of a pair of tunneling doublets. Thus even a moderate electrostatic field can convert second-order alignment by a laser field into a strong pseudo-first-order orientation [8,9]. Our recent study has revealed that a considerably longer turn on (longer than 10 times the rotational period T_{rot}) is necessary to achieve purely adiabatic molecular orientation and the highest possible degree of orientation [15]. After the rapid truncation of the laser pulse at its peak intensity, the molecular orientation is gradually dephased in the laser-field-free condition and is expected to revive at the time of the rotational period of the molecule with the same degree of orientation as that achieved at the peak of the laser pulse.

A rapidly turned-off laser pulse can be shaped with a technique known as a plasma shutter [17]. However, it was a challenge to shape our necessary pulses because both the pulse width (~12 ns) and the pulse energy (~80 mJ) are higher than those used in the previous study [17] by about 2 orders of magnitude. A nanosecond (ns) pulse from an injection-seeded Nd:YAG (yttrium aluminum garnet) laser is collinearly focused by a 500-mm-focal-length lens onto a 50-μm-thick ethylene glycol jet sheet with a femtosecond (fs) laser pulse from a Ti:sapphire-based chirped pulse amplified laser system. At the focus, the peak intensity of the fs pulse is kept well above the threshold of the plasma formation and that of the ns pulse is kept just below the threshold. The timing of the fs pulse is adjusted to arrive at the peak of the ns pulse so that the ns pulse is truncated by the plasma triggered by the fs pulse. The formed plasma is further maintained by the ns pulse energy, and the ns pulse is absorbed by and/or reflected from the plasma after the fs pulse.

Figure 1(a) shows the temporal profile of the shaped pulse measured with a fast photodiode. Since the falling time of the pulse is thought to be much faster than the

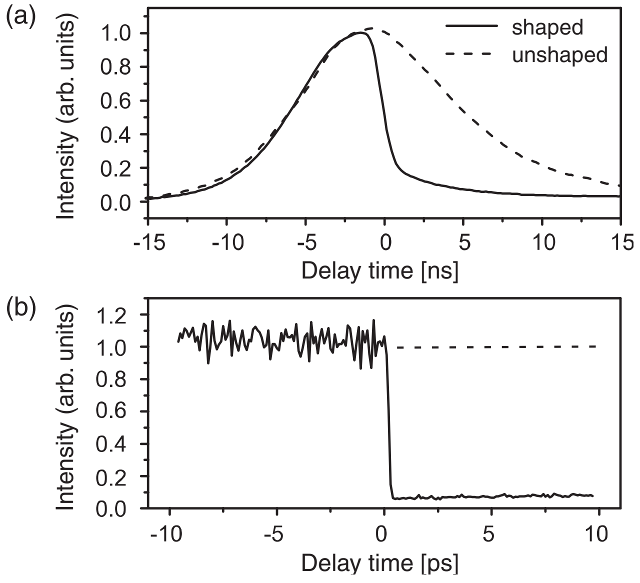

FIG. 1. Temporal evolutions of the shaped pulse measured by (a) a fast photodiode and (b) the sum-frequency generation between the shaped pulse and a portion of the fs pulse in a BBO crystal. The shaped and unshaped pulses are shown by solid curves and dashed curves, respectively. The falling time of the shaped pulse is ~200 fs, and the residual laser field is ~5% in intensity after the truncation of the pulse.

temporal resolution of the measurement (~1 ns), the shaped pulse is further characterized by measuring the sum-frequency signals between the shaped pulse and a portion of the fs pulse generated in a β-BaB_2O_4 (BBO) crystal. For this purpose, the diameter of the fs pulse in the BBO is adjusted to be larger than that of the ns pulse in order to probe the entire transverse section of the shaped pulse. Figure 1(b) shows the intensity profile of the shaped pulse thus measured at around the truncation. The results in Fig. 1 form the evidence that the original 12-ns pulse is truncated with the falling time of ~200 fs though the residual laser field of ~5% in intensity remains, which seems to result from the limited ratio of the focal spot diameter of the fs pulse to that of the ns pulse on the ethylene glycol jet sheet. Although the ratio is limited by the available energy of the fs pulse in the present case, we expect that the perfect truncation with no residual laser field could be achieved if the larger ratio is available. The rising time of ~6 ns, which is much longer than the rotational period $T_{\rm rot} = 82$ ps of an OCS molecule, and the falling time of ~200 fs ensure the adiabatic turn on and the nonadiabatic turn off, respectively [15].

With the rapidly turned-off pulses ($\sim 2 \times 10^{12}$ W/cm^2) thus shaped, we investigate the temporal evolution of alignment and orientation of OCS molecules [10–12]. Alignment and orientation are analyzed by observing fragment ions produced from multiply ionized molecules with the velocity map ion imaging technique and the time-of-flight (TOF) mass spectrometry, respectively. An intense femtosecond probe pulse (~50 fs, 6×10^{14} W/cm^2) is used to multiply ionize the molecules. The shaped pump pulse and the probe pulse are collinearly focused by a 250-mm-focal length lens into the vacuum chamber and crossed at 90° by the supersonic molecular beam, which is supplied by expanding OCS molecules diluted (5%) with argon carrier gas through a 0.25-mm-diameter nozzle and two 0.5-mm-diameter skimmers. The backing pressure is kept 8 atm throughout the present experiments, and the initial rotational temperature is estimated to be ~5 K [10,11].

First we investigate how the molecular alignment created in the adiabatic regime is dephased after the rapid turn off of the shaped pulse and how it revives at $T_{\rm rot}/2$ and $T_{\rm rot}$ of an OCS molecule in the laser-field-free condition. For this purpose, the polarizations of the shaped pulse and the probe pulse are set parallel and perpendicular to the detector plane, respectively, as shown in Fig. 2(a). We observe two-dimensional images of specific fragment ions as a function of the delay (τ) between the shaped pulse and the probe pulse. The specific fragment ion can be selected by gating the microchannel plate (MCP) with a homebuilt pulsed high-voltage power supply. Here we observe CO^+ and S^+ fragment ions produced from OCS^{2+}. A typical ion image thus observed for CO^+ ions at the peak of the pump pulse ($\tau = 0$ ps) is shown in Fig. 2(b). The degree of alignment is evaluated in terms of $\langle \cos^2\theta_{\rm 2D}\rangle$, where $\theta_{\rm 2D}$ is the projection of θ (the polar angle between the shaped

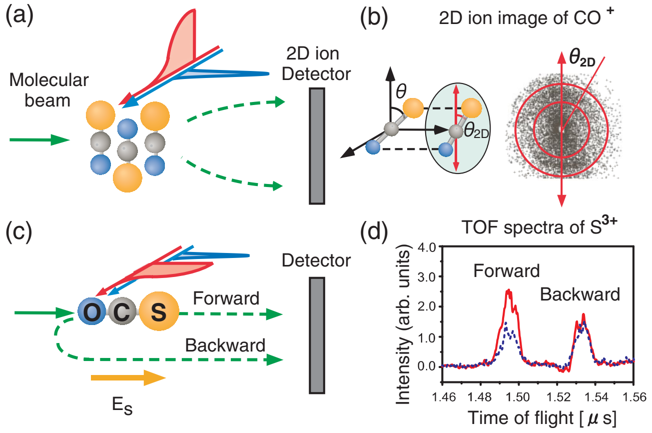

FIG. 2 (color online). (a) Molecular alignment is probed by the two-dimensional ion imaging technique. The polarizations of the shaped pump pulse and the probe pulse are parallel and perpendicular to the detector plane, respectively. (b) An ion image of CO^+ at the peak of the pump pulse. The degree of alignment is evaluated by $\langle \cos^2\theta_{\rm 2D}\rangle$, where $\theta_{\rm 2D}$ is the projection of θ (the polar angle between the pump pulse polarization and the molecular axis) onto the detector plane (see the inset on the left side). (c) Molecular orientation is analyzed by TOF mass spectrometry. The polarizations of the shaped pump pulse and the probe pulse are parallel to the TOF axis. (d) TOF spectra of S^{3+} fragment ions observed with (solid red curve) and without (dashed blue curve) the pump pulse.

pulse polarization and the molecular axis) onto the detector plane [see the inset in Fig. 2(b)]. The fragment ions surrounded by concentric circles as shown in Fig. 2(b) are used for the evaluation of $\langle\cos^2\theta_{2\,\mathrm{D}}\rangle$ to minimize the angular dependence of molecular ionization [18]. When only the probe pulse is employed, the image looks isotropic and $\langle\cos^2\theta_{2\,\mathrm{D}}\rangle$ takes the value of 0.5, ensuring that the molecules are randomly aligned. When the shaped pulse is applied, the molecules are gradually aligned along the pump pulse polarization and $\langle\cos^2\theta_{2\,\mathrm{D}}\rangle$'s are increased to 0.63 ± 0.01 for CO^+ and 0.65 ± 0.01 for S^+ by the peak of the pulse (Fig. 3).

Figure 3 shows the temporal evolutions of $\langle\cos^2\theta_{2\,\mathrm{D}}\rangle$ at around the truncation of the pump pulse, $T_{\mathrm{rot}}/2$, and T_{rot}. Each data point of $\langle\cos^2\theta_{2\,\mathrm{D}}\rangle$ is evaluated from the image accumulated by 1000 laser shots and is measured at the interval of 100 fs. After the truncation of the pump pulse, $\langle\cos^2\theta_{2\,\mathrm{D}}\rangle$ gradually decreases from ~ 0.65 to ~ 0.53. At around $T_{\mathrm{rot}}/2$, $\langle\cos^2\theta_{2\,\mathrm{D}}\rangle$ modulates and decreases down to ~ 0.47, indicating that the molecules are antialigned and localized in the plane perpendicular to the pump pulse polarization. At around T_{rot}, $\langle\cos^2\theta_{2\,\mathrm{D}}\rangle$ revives, and the latter half of the modulation looks like that just after the truncation of the pump pulse. The slightly reduced value of $\langle\cos^2\theta_{2\,\mathrm{D}}\rangle$ (~ 0.6) is most likely due to the effect of the residual laser field. The characteristic modulations of $\langle\cos^2\theta_{2\,\mathrm{D}}\rangle$ at the three temporal regions are in good agreement with theoretical calculations of degree of alignment $\langle\cos^2\theta\rangle$, which forms firm evidence that the alignment of OCS molecules has been gradually dephased after the rapid truncation of the pump pulse and revived at $T_{\mathrm{rot}}/2$ and T_{rot} in the laser-field-free condition. Here we further note that $\langle\cos^2\theta_{2\,\mathrm{D}}\rangle$ keeps the value of ~ 0.53 except for the three temporal regions discussed above. This increase of $\langle\cos^2\theta_{2\,\mathrm{D}}\rangle$ from 0.5 is a clear signature of permanent alignment of rotational wave packets created by the time of the peak of the shaped pulse.

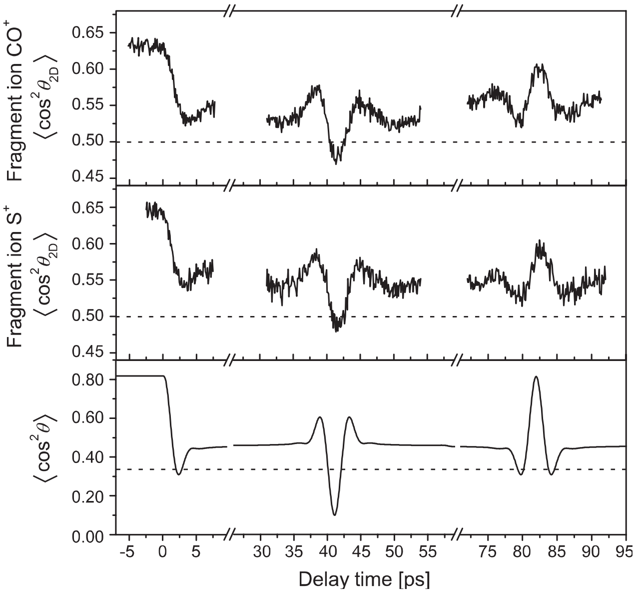

FIG. 3. The temporal evolutions of $\langle\cos^2\theta_{2\,\mathrm{D}}\rangle$ for CO^+ (top panel) and S^+ (middle panel) at around the truncation of the pump pulse, $T_{\mathrm{rot}}/2$, and $T_{\mathrm{rot}}(= 82$ ps). The bottom panel shows the calculations of the degree of alignment $\langle\cos^2\theta\rangle$, where θ is the polar angle between the pump pulse polarization and the molecular axis.

Next we examine how the molecular orientation created in the adiabatic regime is dephased after the rapid turn off of the shaped pulse and how it revives at T_{rot} of an OCS molecule in the laser-field-free condition. The molecular orientation is probed by TOF mass spectrometry [Fig. 2(c)] with the polarizations of both the shaped pulse and the probe pulse perpendicular to the detector plane, i.e., parallel to the TOF axis. The acceleration field (800 V/cm) of the TOF mass spectrometer, which is negligible compared to a laser field (~ 40 MV/cm for 2×10^{12} W/cm^2), serves also as an electrostatic field to orient the molecules. Since the apparatus is originally designed for two-dimensional ion imaging, a 5-mm-diameter aperture is placed in front of the MCP detector when it is used as a TOF mass spectrometer.

Here we focus on the S^{3+} fragment ions produced from OCS^{5+} and/or OCS^{6+} ([16] in Ref. [10]). When the polarization of the probe pulse is parallel to the TOF axis, a pair of peaks appears in the TOF spectrum of S^{3+} as shown in Fig. 2(d). The "forward" ("backward") peak corresponds to the fragment ions emitted toward (against) the detector, which means that the S atoms in the OCS molecules are directed toward (away from) the detector at the instant of dissociation. Without the pump pulse, the two peaks look almost symmetric as shown by the dashed blue curve in Fig. 2(d), which confirms that the molecules are randomly oriented and nonadiabatic orientation induced by the intense femtosecond probe pulse is negligible. On the other hand, when the pump pulse is applied, the two peaks become asymmetric, which we interpret as the result that more than half of the OCS molecules are oriented with their S atoms directed toward the detector. In fact, since the permanent dipole moment of an OCS molecule is directed toward the S atom, the molecules tend to be oriented with their S (O) atoms directed toward (against) the direction of the electrostatic field, i.e., toward (against) the detector. Our observation shown in Fig. 2(d) is consistent with this expectation.

As a measure of the degree of orientation, we employ a parameter $\mathrm{FB} \equiv (I_f - I_b)/(I_f + I_b)$, where I_f and I_b are the integrated signals of the forward and the backward fragment ions, respectively. In the case of OCS, the FB parameter for S^{3+} ions and the orientation cosine $\langle\cos\theta\rangle$ behave in the same way. In fact, when the molecules are randomly oriented or only aligned, both the FB parameter and $\langle\cos\theta\rangle$ take the value of 0, while both of them take the value of 1 (-1) when the molecules are completely ori-

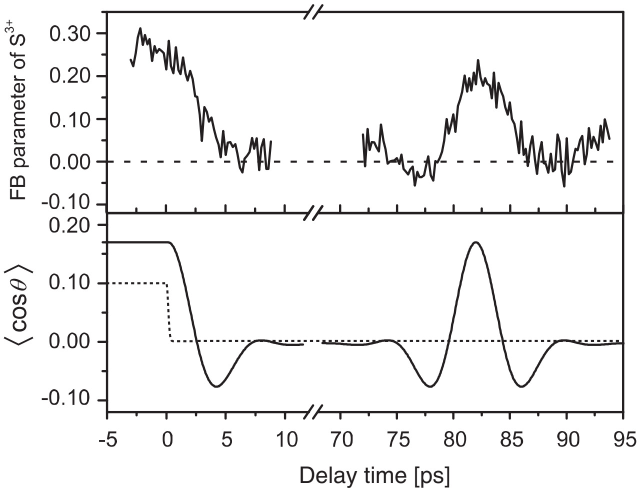

FIG. 4. The upper panel shows the temporal evolutions of the FB parameter for S^{3+} fragment ions at around the truncation of the pump pulse and $T_{\mathrm{rot}}(= 82$ ps). The lower panel shows the calculations of the degree of orientation $\langle\cos\theta\rangle$, where θ is the polar angle between the electrostatic field and the permanent dipole moment of an OCS molecule. The intensity profile of the shaped pump pulse is also represented by a dotted curve in the lower panel.

ented in the right (wrong) way. As shown in Fig. 2(d), FB = 0 when only the probe pulse is applied, and FB = 0.26 when the pump pulse is applied in the presence of an electrostatic field.

Figure 4 shows the temporal evolutions of the FB parameter at around the truncation of the pump pulse and T_{rot}. Each data point of the FB parameter is evaluated from the TOF spectrum accumulated by 5000 laser shots and is measured at the interval of 200 fs. After the truncation of the pump pulse, the FB parameter gradually decreases from 0.28 to 0. At around T_{rot}, the FB parameter revives, and the latter half of the modulation looks like that just after the truncation of the pump pulse [19]. The slightly reduced value of the FB parameter (~0.21) seems to be due to the same reason as that for molecular alignment mentioned above. The characteristic modulations of the FB parameter at the two temporal regions are in good agreement with theoretical calculations of the degree of orientation $\langle\cos\theta\rangle$, which forms firm evidence that the orientation of OCS molecules has been gradually dephased after the rapid truncation of the pump pulse and successfully revived at T_{rot} in the laser-field-free condition.

The present technique could be extended to laser-field-free three-dimensional molecular orientation [15]. As shown in Fig. 4, the temporal evolution of both alignment and orientation is much slower than the truncation of the laser pulse. Therefore, by employing an intense nonresonant shaped laser field with elliptical polarization instead of linear polarization in the presence of an electrostatic field, laser-field-free three-dimensional alignment and orientation could be achieved just after the truncation of the pump pulse [12,20].

In conclusion, we have demonstrated nonadiabatic laser-field-free orientation of OCS molecules by employing an intense nonresonant rapidly turned-off laser field in the presence of a moderate electrostatic field. For this purpose, we have developed a technique to truncate a 12-ns 100-mJ-class laser pulse at its peak to have the falling time of ~200 fs. This accomplishment means that a new class of molecular sample is now available for various applications in stereodynamics in chemical reactions, electronic stereodynamics, ultrafast molecular imaging, attosecond science, surface science, and so on.

The authors are grateful to Mr. Taro Itatani (National Institute of Advanced Industrial Science and Technology, Tsukuba, Japan) for his help in the preparation of the liquid circulation system. This work was supported by Grants-in-Aid No. 14102012 and No. 19204041 from the Japan Society for the Promotion of Science (JSPS).

---

*hsakai@phys.s.u-tokyo.ac.jp

[1] H. Stapelfeldt and T. Seideman, Rev. Mod. Phys. **75**, 543 (2003).
[2] T. Seideman and E. Hamilton, Adv. At. Mol. Opt. Phys. **52**, 289 (2006).
[3] Special issue on Stereodynamics of Chemical Reactions [J. Phys. Chem. A **101**, 7461 (1997)].
[4] D. Herschbach, Eur. Phys. J. D **38**, 3 (2006).
[5] M. Lein, J. Phys. B **40**, R135 (2007).
[6] P. Lan *et al.*, Phys. Rev. A **76**, 021801(R) (2007).
[7] H. Hou *et al.*, Science **277**, 80 (1997).
[8] B. Friedrich and D. Herschbach, J. Chem. Phys. **111**, 6157 (1999).
[9] B. Friedrich and D. Herschbach, J. Phys. Chem. A **103**, 10 280 (1999).
[10] H. Sakai *et al.*, Phys. Rev. Lett. **90**, 083001 (2003).
[11] S. Minemoto *et al.*, J. Chem. Phys. **118**, 4052 (2003).
[12] H. Tanji *et al.*, Phys. Rev. A **72**, 063401 (2005).
[13] M. Machholm and N.E. Henriksen, Phys. Rev. Lett. **87**, 193001 (2001).
[14] M. Spanner *et al.*, Phys. Rev. Lett. **92**, 093001 (2004).
[15] Y. Sugawara *et al.*, Phys. Rev. A **77**, 031403(R) (2008).
[16] A.A. Radzig and B.M. Smirnov, *Reference Data on Atoms, Molecules, and Ions* (Springer-Verlag, Berlin, 1985).
[17] B.J. Sussman *et al.*, Phys. Rev. A **73**, 053403 (2006).
[18] T. Suzuki *et al.*, Phys. Rev. Lett. **100**, 033603 (2008).
[19] Furthermore, we have confirmed that the FB parameter for a counterpart fragment such as O^{2+} modulates out of phase with that for S^{3+}.
[20] J.J. Larsen *et al.*, Phys. Rev. Lett. **85**, 2470 (2000).